Proceedings of the NROCK 2023
The IV Nordic Symposium on
Rock Mechanics and Rock Engineering
ISBN 978-9935-9436-2-0
DOI 10.33112/nrock2023.7

Quantitative numerical assessment of blast-induced wall damage

Marie-Hélène Fillion (mfillion@laurentian.ca)

O. Karimi
Laurentian University, Sudbury, Canada
M.-H. Fillion
Québec Ministry of Transportation, Québec, Canada
Laurentian University, Sudbury, Canada
P. Dirige
Workplace Safety North, Sudbury, Canada
Laurentian University, Sudbury, Canada

ABSTRACT

One of the cost-effective methods used for rock breakage in mining is drilling and blasting. In open pit mining, blast-induced damage can reduce the level of stability of benches and pit slopes, which is a concern for the safety of mine personnel. Rock fracturing and fragmentation by blasting is the result of the coalescence of existing and new fractures (created by the blast) in the rock mass. The stress waves affect the rock mass in a few milliseconds while the effects of gas pressure last in the scale of hundreds of milliseconds and have a greater effect on rock fragmentation. The presence of in-situ fractures can have a significant impact on the extent of blast-induced damage beyond the intended area of the blast. These fractures are generally preferential paths of least resistance for the explosive energy. It is therefore necessary to account for the effect of the in-situ fracture network to reliably characterize fracture development and blast-induced damage. Discrete fracture networks (DFN) are representations of joint systems and can estimate the distribution of in-situ fractures within a rock mass. The combined finite (FEM)/discrete (DEM) element method (or FDEM) is a useful tool to simulate the complex rock blasting process. FEM is used for calculating stress distribution and displacements before fracturing (static phase) and, once the fracture process begins, DEM is used for simulating the fractured medium (large displacement phase). The principal objective of this paper is to develop a DFN-based numerical FDEM model to assess the influence of gas pressure on blast-induced damage using a propagating boundary condition, which simulate the effect of gas pressure on a growing network of fractures. A two-holes open pit bench blast was simulated in 2D environment. In this simulation, gas pressure was applied on a propagating boundary (boundary of developed fractures). The numerical model is simulated based on rock and blast properties obtained from an operating open pit mine. The level of blast-induced damage was quantified based on the area of the blast damage zone and the intensity of blast-induced fractures. The results show that the propagating boundary condition provides a realistic simulation of blast holes interaction and blast-induced fracture development.

KEYWORDS

Blast-induced damage; Wall damage; Discrete Fracture Network; Combined finite/discrete element method; Fracture intensity.

INTRODUCTION

In open pit mine operations, drilling and blasting is a widely used method for rock breakage. The desired outcome for blast design could be fragment size, muck-pile shape, direction of displacement, minimizing fly rocks, and/or minimizing damage to final walls (Hall, 2015; International Society of Explosives Engineers, 2011). Insufficient knowledge of the rock properties and in-situ joints characteristics can cause delays and safety concerns in an open pit mine operation due to inadequate rock fragmentation, fly rocks and wall damage.

Wall damage is the extension of cracks and creation of new fractures beyond the intended area of fragmentation, and this can result in instabilities and hazardous environment. This could lead to loss of production, slope failures, damage to equipment and staff injuries (Silva et al., 2019). The blasting outcomes, such as blast-induced damage, are difficult to predict due to the complexity of the blasting process (Mitelman & Elmo, 2014). A good knowledge of the structural features (e.g., in-situ fractures networks) and reliable numerical simulations of the blasting process can aid in overcoming these challenges. Moreover, since the blasting process starts from a static phase to a large displacement phase, modeling should include both continuum and discontinuum models for better representation of the blasting process (Han et al., 2020).

1. DISCRETE FRACTURE NETWORKS

The rock mass consists of one or more rock types and natural fractures. Blast-induced rock fragmentation and wall damage are influenced by these fractures. The fractures act as planes of weakness allowing for the explosive energy to dissipate. Moreover, the in-situ fractures provide venting paths for the explosion gases. Therefore, the fractures should be represented in the blasting simulations. Discrete Fracture Networks (DFN) are 3D representations of joint systems that can estimate the distribution of in-situ block sizes based on field measurements of the fracture properties, i.e., fracture orientation (dip and dip direction) and intensity; and using statistical distributions. The P_{ij} system (Table 1) was introduced by the DFN community as a straightforward way to characterize DFN models in terms of scales and dimensions. The index *i* stands for dimension of sample and the index *j* represents dimension of measurement (Elmo et al., 2014b; Rogers et al., 2009). P32 (fracture area per unit volume) is the preferred measure of the fracture intensity since it represents a non-directional intrinsic measure of fracture intensity (Elmo et al, 2014a). A DFN-based analysis relies on quantifiable joints properties and provides realistic fracture networks with the key advantage of preserving the real joint properties during the modelling process.

Table 1. The Pij system of fracture intensity (Rogers et al., 2009).

		Dimension of Measurement				
		0	1	2	3	
Dimension of Sample	1	P10 No of fractures per unit length of borehole	P11 Length of fractures per unit length			Linear Measures
	2	P20 No of fractures per unit area	P21 Length of fractures per unit area	P22 Area of fractures per area		Areal Measures
	3	P30 No of fractures per unit volume		P32 Area of fractures per unit volume	P33 Volume of fractures per unit volume	Volumetric Measures
Term		Density		Intensity	Porosity	

The DFN model used in this paper was generated using Fracman (Golder Associates, 2020). Table 2 presents the orientation properties (dip and dip direction) of three fracture sets obtained from an open pit mine operated by Iamgold. The P32 value for the input data was calculated based on P21 (length of fractures per unit area) value (Elmo et al., 2014a). Then, using input parameters such as the dispersion of the orientation cluster (Fisher's constant K) and the volumetric fracture intensity P32 (Table 3), the DFN model in the dimensions of 54m long (X axis) × 24m wide (Y axis) × 20m deep (Z axis) was generated (Figure 1a). The length and width of the model were chosen to match the size of the numerical modeling geometry, which represents an open pit bench blast. The bench geometry was extended in length and in width to prevent unrealistic damage when stress waves reach the side and bottom boundaries. Fractures are generated as circular planes and the DFN volume is large enough to reliably represent these fractures. Since the blasting simulation is in 2D environment, a 2D longitudinal section of the 3D DFN model was extracted to represent the intersecting fractures within the rock mass (Figure 1b). These fractures were imported as an input to the developed FDEM model for the blasting scenario.

The orientation data were verified against the input orientation data using DIPS (Rocscience Inc., 2021). Figure 2a presents the stereonet of the input fracture orientation data and Figure 2b illustrates the orientation of the DFN generated fractures. Table 4 compares the input fracture orientation data with the orientation of the DFN generated fractures and their percentage of variation. According to the joint properties database, a variation of +/- 10 degrees in dip direction was observed in surveyed fracture set J1. This fracture set is subvertical which leads to higher variation in dip direction for the DFN generated fractures. Therefore, a more significant variation (14.7%) in dip direction obtained from the DFN model was observed. Based on the percentage of

variation, the significant variation in dip for fracture set J10 (25.0%) is considered acceptable because it is due to a low dip value and the actual variation is one degree. Most of the orientation values fall under 5% variation.

Table 2. Fracture sets properties.

Parameters	Value per Fracture Set		
	J1	J2	J10
Dip (°)	85	41	4
Dip Direction (°)	95	269	96

Table 3. Input data for DFN model generation.

Parameters	Value
Fisher's K	60
P32 (1/m)	0.52

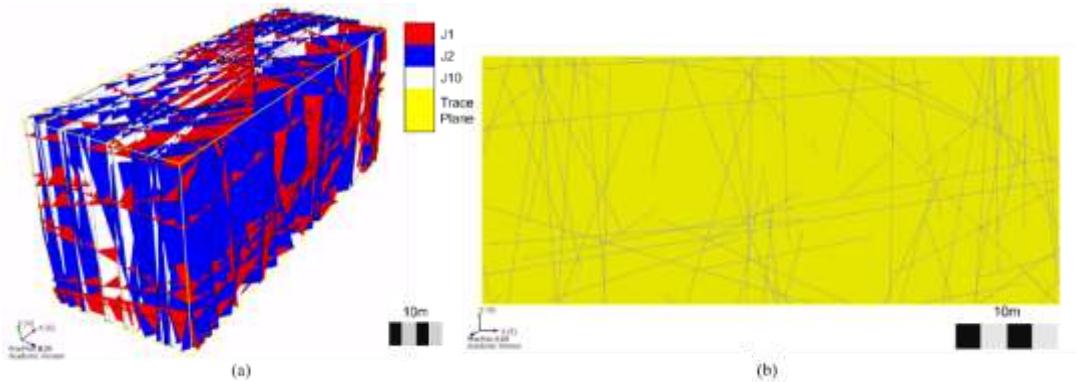

Figure 1. DFN model in Fracman (Golder Associates, 2020): (a) 3D DFN model, (b) 2D longitudinal section.

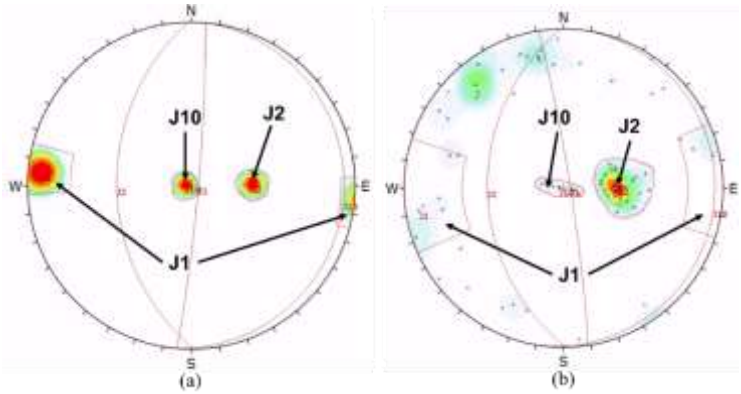

Figure 2. Orientation comparison using DIPS (Rocscience Inc., 2021): (a) Stereonet with input fractures' orientation, (b) Stereonet with DFN generated fractures.

Table 4. Fracture orientation comparison.

	Input Orientation		DFN Generated Orientation		Variation (%)	
Fracture Sets	Dip (°)	Dip Direction (°)	Dip (°)	Dip Direction (°)	Dip	Dip Direction
J1	85	95	84	81	1.2	14.7
J2	41	269	39	269	4.9	0.0
J10	4	96	3	98	25.0	2.1

2. BENCH BLAST NUMERICAL SIMULATION

This paper focuses on the wall damage assessment in terms of blast-induced fracture intensity using a propagating boundary condition to implement the effect of gas pressure within existing and blast-induced fractures. The simulation includes DFN-generated fractures to represent the role of in-situ fractures in the development and propagation path of blast-induced fractures. The bench blast scenario was simulated in 2D environment. The numerical model was developed based on blast design properties obtained from an open

pit mine operated by Iamgold. The DFN model described in Section 1 was used as the input for the simulated scenario. Section 2.1. describes the numerical tool used for simulating the blasting scenario. Section 2.2 details the bench and blast design geometries. Section 2.3 provides the input parameters and material properties used in this analysis. Section 2.4. presents the detonation and gas pressures formulation and how these pressures were applied to the blastholes as pressure boundaries. Finally, Section 2.5. presents the blast damage assessment method.

2.1. Combined Finite/Discrete Element Method (FDEM)

The numerical simulation of the rock mass could be categorized depending on its behavior: continuous or discontinuous approaches (Elmo et al., 2013; Hamdi et al., 2014). For the continuum mechanical problems, the FEM is widely used for simulating large domains or fracture propagation (Hazay & Munjiza, 2016; Jing, 2003). The discrete element method (DEM) is the most used method for discontinuum problems such as fluid flow in fractured medium or large displacements caused by blasting (Hazay & Munjiza, 2016; Zhang, 2016).

Once rock blasting is initiated, the rock mass receives a dynamic load, which results in fracture development, rock fragmentation and muckpile formation. The fragmentation process consists of the detonation of explosives (detonation pressure), creating stress waves in the rock mass to initiate expansion and opening of existing fractures, and new cracks formation. Cracks expand and propagate because of the expansion of explosive gases (gas pressure) and the coalescence of the fractures forms rock fragments. When the fragmented rocks are being ejected because of the gas expansion, the movement is large enough and cannot be modeled with continuum approaches. Neither FEM-only or DEM-only approaches are adequate for simulating rock fragmentation by blasting.

The combined finite-discrete element method (FDEM), which was proposed by Munjiza et al. (1995) and Munjiza (2004), is an advantageous method that combines the finite and discrete element methods (Sun et al., 2016). This method can be used for numerical modeling of the processes that transition from continuum to discontinuum media by incorporating the contact detection interface analysis, as well as fracture creation and propagation (Hazay & Munjiza, 2016; Sun et al., 2016). For modeling the blasting process, FEM is used for calculating stress distributions and displacements in rock before fracture development. Once the fracture process begins, DEM is used for the fractured medium (Zhang, 2016).

2.2. Simulated Blasting Model

To represent blasthole interaction during the blasting process, a two-blastholes open pit bench blast was modeled using Irazu 2D (Geomechanica Inc., 2022). The 2D simulation is faster to simulate in terms of computational time. The scenario simulated for this paper use the DFN model described in Section 1 as an input to the FDEM simulation, as well as rock, blast design and explosive properties which are discussed in Section 2.3. The geometry of the simulated scenario is presented in Figure 3.

There are various studies in the literature regarding the numerical simulation of stress waves only or peak explosive pressure on boundaries of blastholes and their effects on fracture initiation and propagation (Wang et al., 2018). However, due to the complexity of the blasting process, there is limited information about the role of in-situ fractures and gas pressure in the propagating path of blast-induced fractures (Wang et al., 2018). In this simulation, the detonation and gas pressures are applied to the blastholes' boundaries as separate pressure boundaries and the propagating boundary condition developed by Geomechanica Inc. is used to represent the gas pressure within the blast-induced fractures.

The side boundaries of the rock domain are free to move in the vertical (Y) direction, i.e., towards the free surface representing the top of the bench. The bench face is free to move in the vertical (Y) and horizontal (X) direction and the bottom boundary is fixed to its location to represent confined ground. These constraints are used to prevent from generating any unrealistic displacement values near these boundaries. The mesh size progressively increases from 10cm (surrounding the blastholes) to 2m (at the rock boundaries). This progressive increase in mesh size allows for a higher resolution in areas experiencing large magnitudes of stresses and displacements, while lowering the computation time at a larger distance from the blastholes. The horizontal and vertical lengths are exaggerated to remove the effect of unrealistic extra damage near the model boundaries.

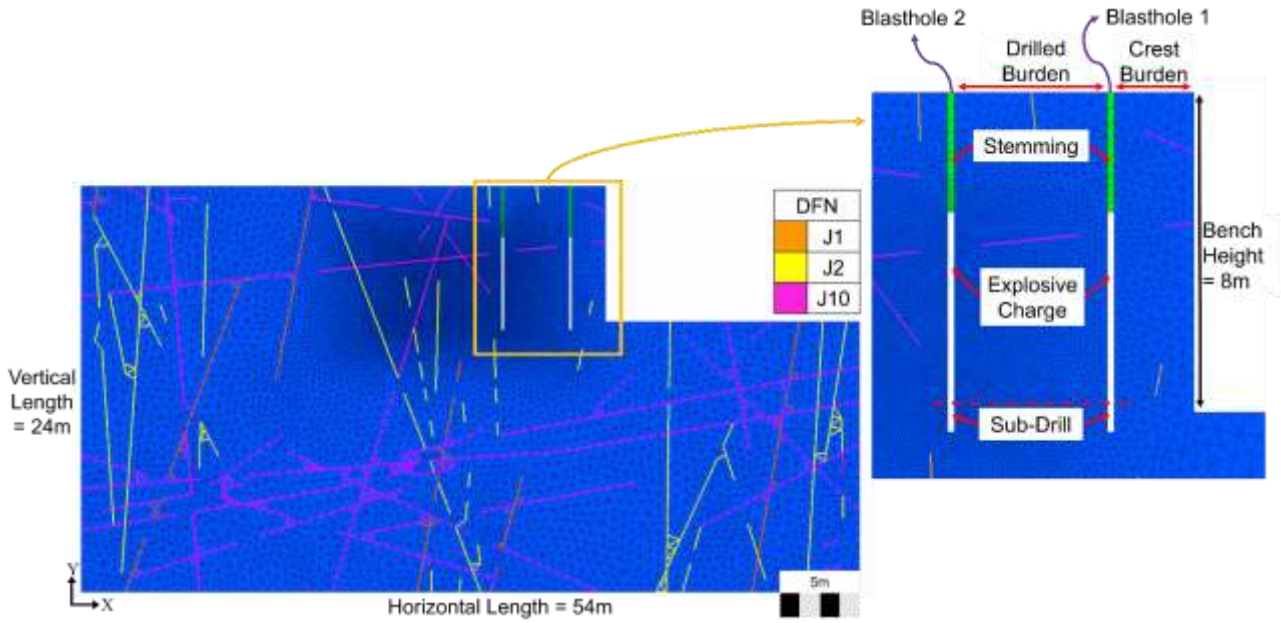

Figure 3. Geometry of the simulated model.

2.3. Material and Blast Design Properties

The rock properties, blast design parameters and explosive properties used in the simulation were obtained from an operating open pit mine. The bench is excavated in a hard rock formation. The required properties for a FDEM simulation are presented in Table 5. The fracture energies for Mode I and II were calculated based on the formulations presented by Whittaker et al. (1992). Table 6 presents the blast design parameters used in developing the numerical model geometry illustrated in Figure 3. The mine site uses a bulk explosive (mixture of ANFO and emulsion also known as heavy ANFO) which is manufactured on site (Table 7). The bulk explosive is considered fully coupled. Finally, the fractures in the DFN model are considered broken which defines them as pure frictional discontinuity surfaces (Geomechanica Inc., 2022). Table 8 presents the values assigned to the DFN model imported to the blasting simulation. The friction coefficient is the tangent of equivalent internal friction angle which was obtained from the mine's geotechnical database.

Table 5. Rock properties for FDEM simulation.

Parameters	Value	Symbol
Density (kg/m^3)	2700	ρ
Young's Modulus (GPa)	60	E
Poisson's Ratio	0.25	υ
Cohesion (MPa)	22	C
Tensile Strength (MPa)	11	f_t
Friction Coefficient	0.47	f_r
Friction Energy Mode I (N/m)	31	G_I
Friction Energy Mode II (N/m)	310	G_{II}
Constitutive Law	Plane strain	

Table 6. Blast design parameters.

Parameters	Value
Crest burden (m)	2
Drilled burden (m)	4
Stemming Length (m)	3
Charge Length (m)	5
Subdrill (m)	0.5
Blasthole diameter (mm)	165
Bench height (m)	8
Inter-Row delay (ms)	142

Table 7. Explosive properties.

Parameters	Value
Explosive Type	Heavy ANFO
Density (kg/m^3)	1200
Velocity of detonation (VOD) (m/s)	5000

Table 8. Fracture properties for DFN.

Parameters	Value
Fracture type	Broken
Friction Coefficient	0.73

2.4. Blasting Pressure Boundary Formulation

The formulation for the maximum detonation pressure within a borehole used in this paper was presented by Hajibagherpour et al. (2020) (Eq. 1).

$$P_d = \frac{4.18\times10^{-7}\times\rho_e\times VOD^2}{1+0.8\rho_e} \times \left({}^{d_c}/_{d_h}\right)^{2.4} \quad (1)$$

Where P_d is the detonation pressure (Pa), VOD is velocity of the detonation (m/s), ρ_e is explosive density (g/cm^3), d_c is explosive diameter (mm), and d_h is blasthole diameter (mm). Since the explosives are considered fully coupled (d_c/d_h=1), Eq. 1 could be written as Eq. 2:

$$P_d = \frac{4.18\times10^{-7}\times\rho_e\times VOD^2}{1+0.8\rho_e} \quad (2)$$

A pressure-time curve is required to apply the detonation pressure with regards to time steps for FDEM analysis. Eq. 3 presents the formulation to determine pressure as a time function (Hajibagherpour et al, 2020).

$$P_t = 4P(e^{-\frac{\beta t}{\sqrt{2}}} - e^{-\sqrt{2}\beta t}) \quad (3)$$

Where P_t is the time history of the dynamic load imposed on blasthole boundary (Pa), P is the maximum detonation/borehole pressure (Pa), β is damping factor (1/s), and t is time (s). β is calculated using Eq. 4 (Hajibagherpour et al, 2020).

$$\beta = -\sqrt{2}\frac{\ln(1/2)}{t_r} \quad (4)$$

Where t_r is the rise time (time of peak pressure). This parameter is calculated by maximum velocity in different media and length of the media (Hajibagherpour et al, 2020). Lu et al. (2012) presented Eq. 5 to calculate the rise time:

$$t_r = \frac{L_e}{VOD} \quad (5)$$

Where L_e is the length of the column charge (m).

The peak gas pressure (borehole pressure) generated after a blast could be calculated using Eq. 6 (Zou, 2017):

$$P_b = 0.12 f_c^n \rho_e VOD^2 \quad (6)$$

Where P_b is borehole pressure (Pa), VOD is velocity of detonation (m/s), ρ_e is the density of explosive, f_c is coupling factor (ratio of the volume of the explosive to the volume of the blasthole excluding the stemming column), and n is coupling factor exponent (value between 1.2 and 1.3 for dry holes and 0.9 for holes filled with water). For a fully coupled explosive, f_c=1 and Eq. 6 could be written as Eq. 7:

$$P_b = 0.12\rho_e VOD^2 \quad (7)$$

Using the available explosive properties (Table 7), the peak detonation pressure is 6.73GPa and the peak gas pressure is 3.36GPa. Using Equations 3 and 4, the detonation and gas pressure-time curves for both blastholes were calculated. Figure 4 depicts the blasting curves applied to both blastholes. Blasthole 2 has the same pressure-time curves with an addition of 142ms delay timing which represents the inter-row delay.

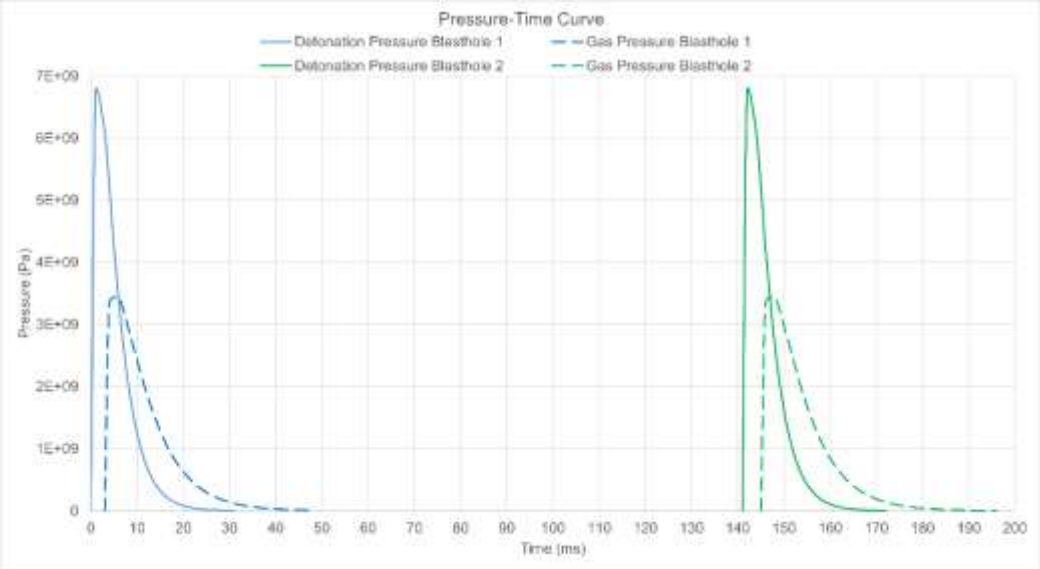

Figure 4. Detonation and gas pressure-time curves.

2.5. Damage Intensity Formulation

To assess and compare the intensity of blast-induced damage in the final wall area, the damage intensity index, D_i, presented by Lupogo et al. (2014) was used. The damage intensity index is defined in Equation 8. Since the focus of this research is to determine the damage intensity in the final wall, D_i was assessed for the back wall area (blast damage zone).

$$D_i = {Yielded\ area}/{Total\ area} \tag{8}$$

where *Total Area* is the area of the blast damage zone (red and yellow boundaries in Figure 5), and *Yielded Area* is the summation of fractured elements areas in the desired section (Figure 6). The yielded elements are the elements that are neighboring a fracture initiated or propagated during the blast.

Two domains for the total area were considered for the model: (1) Domain 1 (red boundary) which includes heavily damaged, partially damaged, and lightly damaged rock mass, and (2) Domain 2 (yellow boundary) which encompasses heavily damaged and partially damaged rock mass. Domain 1 covers 55m^2 and Domain 2 has a total area of 22m^2.

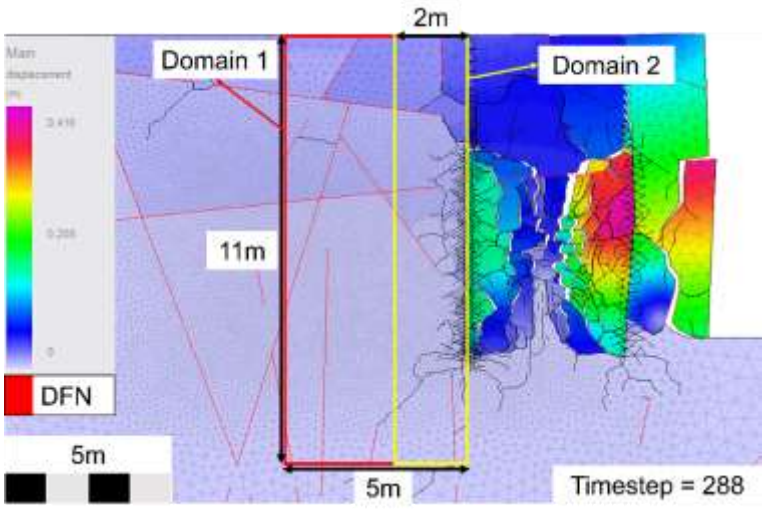

Figure 5. Total Areas selected for the blasting simulations (Domain 1 in red and Domain 2 in yellow).

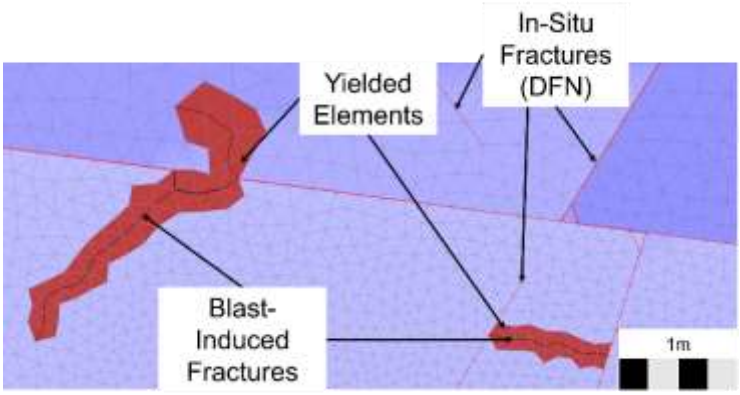

Figure 6. Example of yielded elements (highlighted in red).

3. SIMULATION RESULTS AND BLAST DAMAGE ASSESSMENT

The simulation was conducted using Irazu 2D, a FDEM software developed by Geomechanica Inc. (2022). Section 3.1. presents the simulation results for a propagating boundary condition applied to the boundaries of the blastholes and of the blast-induced fractures to represent gas expansion during the blasting process. In Section 3.2. the damage intensity of the bench wall is assessed.

3.1. Blast Simulation with Propagating pressure boundary

The pressure-time curves for detonation and gas pressures, as depicted by Figure 4, were applied as boundary conditions in this numerical simulation. Figure 7 illustrates the results obtained at three different timesteps during the blasting process. First, the detonation pressure is applied to the external boundary of the two blastholes. Figure 7a shows the fractures generated shortly after blast initiation, when the detonation pressure damages the surrounding rock and generate the initial fractures, transversally to the blasthole boundary. Shortly after blast initiation, the gas pressure is applied on the boundary of blast-induced fractures using the propagating boundary condition developed by Geomechanica Inc. (2022). With this condition, gas flow is considered adiabatic since the gases expand rapidly within the fractures with no heat loss (Zhang, 2016). The pressure is applied on the fractures' boundary until the fractures reach to the radius of the pressure front and/or the pressure reaches zero by the timesteps defined (see Figure 4). Figure 7b illustrates the propagation of blast-induced fractures and the coalescence of these fractures with the closest in-situ fractures represented by the DFN (red fractures in Figure 7). Figure 7b also represents the coalescence of blast-induced fractures between the two blastholes, as well as the timestep for which fractures reach the free face, with the associated increase in displacement. Then, as a result of fracture propagation and gas expansion, rock fragments are formed, and significant displacements are observed (Figure 7c). At the timestep of Figure 7c, venting of the explosion gases has occurred, and no additional damage is observed in the final wall area (i.e., left side of blasthole 2). Since the focus of this paper is wall damage intensity, the numerical simulation is stopped after reaching the large displacement stage shown in Figure 7c.

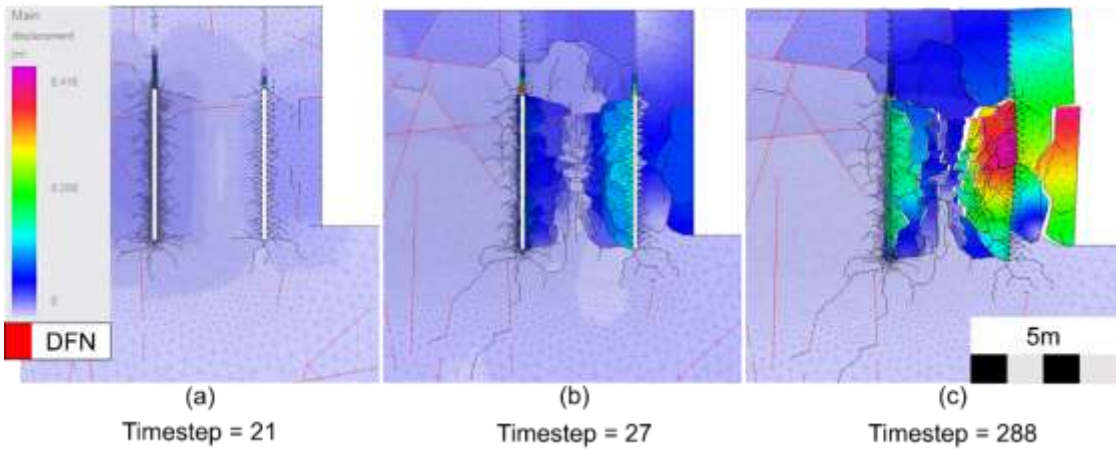

Figure 7. Blasting simulation using a propagating boundary condition: (a) Fracture initiation, (b) Fractures reach the free face, and (c) Rock fragmentation and displacement.

3.2. Damage Intensity Assessment

The damage intensity index D_i was calculated using Equation 8 for domains 1 and 2, as illustrated in Figure 5. Table 10 presents the damage intensity values calculated from the results of the blast damage simulation. The D_i value comparison between domains 1 and 2, shows that the damage intensity for domain 2 is slightly higher than domain 1. This was expected because domain 2 covers a smaller area and includes a heavily damaged zone in the vicinity of blasthole 2 and a partially damaged zone, as the distance from blasthole 2 increases. As illustrated in Figure 7b and 7c, the fractured rock is mostly focused on half of the drilled burden distance, i.e., in a one-meter distance from blasthole 2.

Table 10. Damage intensity values for domains 1 and 2.

Scenario	Damage Intensity (D_i)	
	Domain 1 (red)	Domain 2 (yellow)
Blast with Propagating Boundary Condition	0.012	0.015

Due to the formulation used for blast damage assessment (Eq. 8), D_i is influenced by the area selected for blast damage assessment and by the resolution (i.e., mesh size) used for the numerical simulation of the blasting process. When comparing multiple blast design scenarios with the suggested blast damage assessment method for blast optimization, the same area and resolution should be used to represent the blast damage zone.

4. CONCLUSION

Blast-induced damage should be minimized to ensure safety for mine personnel and equipment. The results of the blasting simulation demonstrated that in-situ fractures influence the propagation path of blast-induced fractures. Consequently, this will influence the dissipation of explosive energy and explosion gas venting during the blasting process. A sufficient knowledge of in-situ fracture network is needed for reliably assessing the outcome of a blast design. Discrete fracture network (DFN) modelling is a useful tool to represent the characteristics of the fracture network (in-situ fracture orientation and intensity) in numerical simulations of the blasting process, in order to evaluate how these fractures can influence fracture propagation and blast-induced damage. A reliable estimate of the volumetric fracture intensity (P32) is necessary to generate a DFN model representative of the field conditions. The P32 value (area of fractures per unit volume) cannot be measured in the field and is therefore estimated from P10 (number of fractures per unit length of borehole) and/or P21 (length of fractures per unit area). A limited dataset is often one of the limitations in geologically governed simulations. Sufficient and good quality structural data (dip, dip direction, spacing, persistence, etc.) are necessary to generate a representative DFN model.

The results of this study demonstrated that the combined finite-discrete element method (FDEM) is a capable tool to simulate the static and dynamic phases of the blasting process. Despite the advantage of reducing the computational time, a two-dimensional FDEM blasting simulation is limited because it cannot represent the interaction between blastholes on the same row. Blast-induced fracture propagation and fragmentation are three-dimensional processes, and this can have an impact on the resulting wall damage assessment. Moreover, the rock properties should be a primary consideration in blast simulation because, as opposed to blast design parameters (burden, spacing, timing sequence, etc.), rock properties are site-specific and cannot be controlled. A sufficient level of confidence in the rock properties (strength, elastic properties, density, etc.) used for FDEM simulation is then necessary for a reliable wall damage assessment. According to the blasting simulation presented in this paper, the propagating boundary condition used to represent the effect of the gas pressure allowed for a realistic simulation of fracture development, blasthole interaction and formation of rock fragments. The proposed blast damage assessment method can be used to evaluate different blasting scenarios for minimizing wall damage, while reducing the costs of conducting multiple test blasts.

5. ACKNOWLEDGEMENTS

The authors acknowledge the support of the Natural Sciences and Engineering Research Council (NSERC) and Iamgold Corporation for research funding, WSP-Golder for access to the DFN software Fracman, and Geomechanica Inc. for access to the FDEM software Irazu.

REFERENCES

Elmo, D., Liu, Y., & Rogers, S. (2014a). Principles of discrete fracture network modelling for geotechnical applications. In: Proceedings of the First International DFNE Conference, 19-23 October, Vancouver, British Columbia, Canada. 8 p.

Elmo, D., Rogers, S., Stead, D., & Eberhardt, E. (2014b). Discrete Fracture Network approach to

characterise rock mass fragmentation and implications for geomechanical upscaling. Mining Technology, 123(3), 149–161. https://doi.org/10.1179/1743286314Y.0000000064

Elmo, D., Stead, D., Eberhardt, E., & Vyazmensky, A. (2013). Applications of Finite/Discrete Element Modeling to Rock Engineering Problems. International Journal of Geomechanics, 13(5), 565–580. https://doi.org/10.1061/(ASCE)GM.1943-5622.0000238

Geomechanica, Inc. (2022). Irazu 2D Geomechanical Simulation Software (Computer Software). V.5.1. Theory Manual. Geomechanica Inc., Toronto, ON, Canada. 123 p.

Golder Associates. (2020). FracMan: DFN software suite [Computer software]. Golder Associates, Toronto, ON, Canada. Retrieved from http://www.golder.com/fracman/.

Hajibagherpour, A., Mansouri, H., & Bahaaddini, M. (2020). Numerical modeling of the fractured zones around a blasthole. Computers and Geotechnics, 123, 103535. https://doi.org/10.1016/j.compgeo.2020.103535

Hall, A. (2015). Predicting Blast-Induced Damage for Open Pit Mines Using Numerical Modeling Software and Field Observations (M. A. Sc. Thesis). Laurentian University, Sudbury, Ontario, Canada. https://zone.biblio.laurentian.ca/handle/10219/2930

Hamdi, P., Stead, D., & Elmo, D. (2014). Damage characterization during laboratory strength testing: A 3D-finite-discrete element approach. Computers and Geotechnics, 60, 33–46. https://doi.org/10.1016/j.compgeo.2014.03.011

Han, H., Fukuda, D., Liu, H., Salmi, E., Sellers, E., Liu, T., & Chan, A. (2020). Combined finite-discrete element modelling of rock fracture and fragmentation induced by contour blasting during tunnelling with high horizontal in-situ stress. International Journal of Rock Mechanics and Mining Sciences, 127, 104214. https://doi.org/10.1016/j.ijrmms.2020.104214

Hazay, M., & Munjiza, A. (2016). Introduction to the Combined Finite-Discrete Element Method. In Computational Modeling of Masonry Structures Using the Discrete Element Method, Sarhosis V., Bagi K., Lemos J. & Milani G. (Ed.). IGI Global.: pp. 123-145. doi: 10.4018/978-1-5225-0231-9.ch006

International Society of Explosives Engineers. (2011). ISEE blasters' handbook. (18th ed.). Cleveland, Ohio: International Society of Explosives Engineers.

Jing, L. (2003). A review of techniques, advances and outstanding issues in numerical modelling for rock mechanics and rock engineering. International Journal of Rock Mechanics and Mining Sciences, 40(3), 283–353. https://doi.org/10.1016/S1365-1609(03)00013-3

Lu, W., Yang, J., Yan, P., Chen, M., Zhou, C., Luo, Y., & Jin, L. (2012). Dynamic response of rock mass induced by the transient release of in-situ stress. International Journal of Rock Mechanics and Mining Sciences, 53, 129-141. https://doi.org/10.1016/j.ijrmms.2012.05.001

Lupogo, K., Tuckey, Z., Stead, D., & Elmo, D. (2014). Blast damage in rock slopes: potential applications of discrete fracture network engineering. In Proceedings of the 1st International Discrete Fracture Network Engineering Conference, Vancouver, Canada. p (Vol. 14).

Mitelman, A., & Elmo, D. (2014). Modelling of blast-induced damage in tunnels using a hybrid finite-discrete numerical approach. Journal of Rock Mechanics and Geotechnical Engineering, 6(6), 565–573. https://doi.org/10.1016/j.jrmge.2014.09.002

Munjiza, A. (2004). The combined finite-discrete element method. John Wiley & Sons Ltd., Chichester, UK. doi: 10.1002/0470020180.

Munjiza, A., Owen, D. R. J., & Bicanic, N. (1995). A combined finite-discrete element method in transient dynamics of fracturing solids. Engineering Computations, 12(2), 145–174. https://doi.org/10.1108/02644409510799532

Rocscience Inc. (2021). DIPS Tutorial (version 8) (Computer Software). Available from https://www.rocscience.com/software/dips

Rogers, S., Elmo, D., Beddoes, R., & Dershowitz, W. (2009). Mine scale DFN modelling and rapid upscaling in geomechanical simulations of large open pits. In: Proceedings of the International Symposium on 'Rock Slope Stability in Open Pit Mining and Civil Engineering', November 2009, Santiago, Chile: 11 p.

Silva, J., Worsey, T., & Lusk, B. (2019). Practical assessment of rock damage due to blasting. International Journal of Mining Science and Technology, 29(3), 379-385. https://doi.org/10.1016/j.ijmst.2018.11.003

Sun, G., Sui, T., & Korsunsky, A. (2016). Review of the hybrid finite-discrete element method (FDEM). In: Proceedings of the World Congress on Engineering, 29 June - 1 July 2016, London, U.K., 5 p.

Wang, Y., Wang, S., Zhao, Y., Guo, P., Liu, Y., & Cao, P. (2018). Blast induced crack propagation and damage accumulation in rock mass containing initial damage. Shock and Vibration, 2018. https://doi.org/10.1155/2018/3848620

Whittaker, B.N., Singh, R.N., Sun, G., (1992). Rock Fracture Mechanics: Principles, Design, and Applications (p. 570). Amsterdam: Elsevier.

Zhang, Z.-X. (2016). Rock fracture and blasting: Theory and applications. Elsevier Inc., Cambridge, MA, USA.

Zou, D. (2017). Theory and technology of rock excavation for civil engineering (p. 699). Springer, Singapore.